



ELSEVIER

Available online at www.sciencedirect.com

 ScienceDirect

Proceedings of the Combustion Institute 33 (2011) 3177–3183

Proceedings
of the
Combustion
Institute

www.elsevier.com/locate/proci

Influence of gas-phase reactions on catalytic reforming of isooctane

Torsten Kaltschmitt^{a,b}, Lubow Maier^b, Marco Hartmann^a,
Christian Hauck^a, Olaf Deutschmann^{a,b,*}

^a Institute for Chemical Technology and Polymer Chemistry, Karlsruhe Institute of Technology (KIT),
P.O. Box 6980, 76049 Karlsruhe, Germany

^b Institute for Nuclear and Energy Technologies, Karlsruhe Institute of Technology (KIT), P.O. Box 6980,
76049 Karlsruhe, Germany

Available online 15 September 2010

Abstract

The significance of gas-phase reactions in catalytic partial oxidation (CPOX) of isooctane at short contact times and high temperatures is studied experimentally and numerically to gain further understanding of hydrogen production by CPOX of logistic fuels for on-board applications. Special attention is given to the formation of coke precursors. CPOX of isooctane over a rhodium coated monolith with a molar inlet C/O ratio of 1.1 is used as reference case for a two-dimensional flow field description coupled with detailed surface and gas-phase reaction mechanisms. The results reveal catalyst coking and formation of coke precursors in the oxygen-free catalyst zone. Taking the product composition of the rich operated CPOX reactors (C/O = 1.0–1.6) as inlet composition, homogeneous conversion in the gas-phase is studied in the temperature range from 873 to 1173 K in a plug flow reactor. Conversion in the gas-phase is modeled by two detailed reaction mechanisms. Results show that most of the by-products and soot precursor species arise from unconverted fuel and not from additionally added hydrocarbons like ethylene. Both mechanisms well-predict all experimentally observed trends in gas-phase composition, both in axial reactor profiles and for different inlet compositions. The amount of soot precursors raises with increasing fuel feed corresponding to an increasing C/O ratio in CPOX experiments.

© 2010 The Combustion Institute. Published by Elsevier Inc. All rights reserved.

Keywords: Partial oxidation; Isooctane; Synthesis gas; Reaction kinetics

1. Introduction

Compact and autothermal reformers for the production of hydrogen and synthesis gas (H₂ and

CO) from liquid hydrocarbon fuels such as gasoline, diesel, and kerosene represent an efficient on-board technique for electricity supply via fuel cells (auxiliary power units, APU) as well as primary and secondary measures for reduction of NO_x emissions. Conventional fuels are attractive due to their high energy density, widespread production, and distribution and retailing infrastructure [1]. Among the three reforming routes, i.e. steam reforming (SR), partial oxidation (POX), and autothermal reforming (ATR, combination of SR and

* Corresponding author at: Karlsruhe Institute of Technology (KIT), P. O. Box 6980, 76049 Karlsruhe, Germany. Fax: +0049 721 608 4805.

E-mail address: deutschmann@kit.edu (O. Deutschmann).

POX), SR is less attractive for mobile applications due to slow start-up and endothermic operation [2].

The reformers often consist of monolithic structures with pore diameters on the order of one millimeter coated with noble metal catalysts such as rhodium. Aside from the heterogeneous conversion on the catalytic surface, homogeneous reactions in the gas-phase may be significant at the operating temperatures of approximately 1000 K, in particular for the higher hydrocarbons containing logistic fuels. Coking and aging of the catalyst as well as coke formation downstream the reformer from precursors formed in the reformer are major challenges in practical realizations of on-board reformers and APUs. The formation of coke precursors is contributed to homogeneous gas-phase reactions [3], in particular at fuel rich operating conditions, i.e. molar C/O ratios above unity.

The formation of hydrogen by CPOX of hydrocarbons over Rh is generally accepted to follow the indirect route that means, first total oxidation of the hydrocarbon occurs until most of the oxygen is consumed, at least near the catalytic surface, and then, the remaining fuel is steam-reformed [4–7]. Numerically predicted [8] and experimentally determined [9] axial species profiles implicate complete fuel conversion within the first millimeters of the catalyst channel for lean conditions ($C/O < 1.0$) with H_2 , CO, H_2O , and CO_2 being the only products. However, at $C/O > 1.0$, an increasing amount of by-products such as methane, olefins, and aromatics are detected [10,11], the latter ones indicating thermal decomposition (pyrolysis) of the fuel in the gas-phase [3]. A recent study on CPOX of isooctane revealed the on-set of homogeneous conversion at a point in the reactor, at which oxygen is almost totally consumed and coke is accumulated on the catalyst [12]. At this location, the mixture consists of synthesis gas, steam, and CO_2 and some remaining fuel. Since the product stream cannot be cooled down instantaneous beyond the catalyst, homogeneous gas-phase reactions may continue beyond the catalyst. In case of CPOX of methane Burke and Trimm investigated the coking behavior downstream the catalyst zone with and without nitrogen cooled product gas stream at different pressures. Coke was observed at about 750 kPa but was avoided when gas-phase cooling was employed, even up to 1500 kPa [3]. Consequently, a study on the impact of gas-phase chemistry on conversion and selectivity of CPOX reformers must be carried out at those conditions occurring in the downstream part of the catalyst and in the post-catalyst zone.

The present study focuses on the impact of gas-phase reactions downstream the oxidation zone in a CPOX-reformer for higher hydrocarbon fuels; isooctane is used as model fuel. First, a reference

case with a Rh catalyst operated at rich conditions will be discussed (catalytic case). Then, homogeneous conversion of the product stream, i.e. the remaining (unconverted) fuel and the products of a CPOX reactor, is investigated experimentally and numerically in the fuel rich region downstream the catalyst (non-catalytic case). Numerical simulations using two different gas-phase reaction mechanisms predict the axial species profiles and the product compositions, which are compared with the measured ones.

2. Experimental procedure

2.1. Catalytic case

In the CPOX reactor, a 1 cm long Rh coated monolith is placed in a quartz tube surrounded by a furnace for heating and thermal insulation. The product stream is analyzed by FT-IR, MS, GC/MS, and paramagnetic oxygen detection. Further details are given in recent publications [10,11].

2.2. Non-catalytic case

A quartz tube, 2 cm inner diameter, is placed in a furnace of total length of 25 cm. Thermocouples are placed at the reactor inlet ($z = 0$ m) and centre zone ($z = 0.125$ m) inside the tube. The position of the centered thermocouple corresponds to the location of the catalyst exit in standard CPOX experiments [10] and equates to the highest expected temperature in the tube downstream the catalyst. The experimental setup allows well-defined mixing of liquid fuels with boiling points up to 553 K with the gaseous components; up to eight additional chemical species can be added to the inlet flow. Flow determination for quantification of each species is done by internal standard methods and DryCal[®] technology. Experiments without catalysts were conducted using a simulated exhaust gas of an isooctane fueled CPOX reactor as inlet gas, which consists of mainly synthesis gas, steam, CO_2 , ethylene, and the remaining fuel isooctane (Table 1). This composition is fed to the reactor tube under isothermal conditions and gas-phase products have been quantified for $C/O = 1.0, 1.3, \text{ and } 1.6$. The product stream is analyzed by FT-IR, MS, GC/MS, and paramagnetic oxygen detection [10,11].

Four different temperatures are used to investigate gas-phase reactions and kinetic parameters at isothermal conditions. Furnace temperature is set to 873 K (770 K), 973 K (877 K), 1073 K (993 K), and 1173 K (1108 K) for a measurement of three different C/O ratios of 1.0, 1.3, and 1.6. Values in parentheses are the corresponding temperatures measured inside the reactor tube. Below this temperature gas-phase reactions can be neglected.

Table 1
Inlet compositions given in mole fractions.

C/O	1	1.3	1.6
CO	2.01E-01	1.82E-01	1.68E-01
H ₂	2.32E-01	2.29E-01	2.12E-01
CO ₂	1.10E-02	1.18E-02	1.41E-02
H ₂ O	1.47E-02	8.75E-03	1.34E-02
Ethylene	0.00E+00	4.85E-04	4.41E-04
Isooctane	6.25E-05	2.77E-03	7.68E-03
Nitrogen	5.41E-01	5.65E-01	5.84E-01

For each measurement the furnace is heated to 523 K and the composition of C/O = 1.0 is adjusted. When steady state is reached, C/O is changed to 1.3 and subsequently to 1.6. After that the furnace temperature is set to 873 K with a C/O ratio beginning at 1.0. Once steady state is reached, C/O is changed as described above. After steady state of C/O = 1.6 is reached, a burn-off is conducted (973 K, 15 K/min, 20 min, 1 SLPM Air) for full removal of carbon deposits in the quartz reactor. This procedure is repeated for temperatures from 973 to 1173 K. A constant dilution of 3.2 SLPM nitrogen is used in all experiments, corresponding to the nitrogen feed of the referenced CPOX experiment [10].

3. Modeling approach

Catalytic and non-catalytic conversion of isooctane in the tubular reactor is modeled using a two-dimensional and a one-dimensional flow field description, respectively. Both simulations apply tools of the DETCHEM software package [13], DETCHEM^{CHANNEL} and DETCHEM^{PLUG}, respectively. The DETCHEM^{CHANNEL} code was recently shown to efficiently treat catalytic reforming of logistic fuel surrogates even if thousands of reactions were implemented [14–17]. The catalytic case here serves as reference to illustrate the problem of adequate gas-phase reaction models, which is the focus of the current paper.

3.1. Catalytic case

The reactor is set-up in a way that due to the thermal insulation the temperature gradient across the catalyst is small. Furthermore, uniform inlet conditions are ensured. Therefore, all channels of the monolith behave essentially alike, and one representative channel needs to be analyzed only. The flow field inside the monolith channel is laminar. This single channel is approximated by an axis-symmetric cylinder leading to the axial and radial spatial coordinates as independent variables of the flow field simulation. Due to the short residence time, being on the order of milliseconds, the transport in axial direction is mainly determined by convection implying that axial diffusion can be neglected, which reduces the elliptic

cal structure of the steady-state Navier–Stokes equations to a parabolic one by application of a boundary-layer approximation [18]. At given inlet conditions, the boundary-layer equations are solved by integration along the axial direction through a method-of-lines procedure. The chemical reactions are modeled by detailed reaction schemes for heterogeneous and homogeneous reactions. The state of the catalytic surface is then described by the temperature and a set of locally varying species surface coverages.

Inlet and boundary conditions of the simulation of catalytic partial oxidation of isooctane over Rh are taken from the experiment [10–12], in which a 1 cm long Rh coated monolith was used, fed with 4 SLPM isooctane/oxygen mixture at the catalyst temperature of 1080 K, C/O ratio of 1.1, and 80% N₂ dilution.

3.2. Non-catalytic case

In the simulation of the non-catalytic conversion in a heated tube, inlet and boundary conditions were chosen according to the isothermal experimental study described above and in Table 1. A one-dimensional isothermal plug flow model was applied. The product composition of the catalytic experiment serves now as inlet feed. Since the measured catalyst exit temperature was chosen as reference (in the center of the tube) for the operating reactor temperature in the non-catalytic experiment, the conversion numerically predicted by the simulation can be interpreted as an upper limit of the total conversion in the homogeneous reaction zone downstream the catalyst.

3.3. Surface reaction mechanism

In the catalytic case, a recently developed surface reaction mechanism consisting of 56 reactions among nine gas-phases and 17 surface adsorbed species was used without modification [12].

3.4. Gas-phase reaction mechanisms

In the catalytic case and the non-catalytic case, detailed homogeneous gas-phase mechanisms have been coupled with the flow field description. Two different homogeneous chemistry models for isooctane are used including aromatic (AH) and polyaromatic hydrocarbons (PAH) to better indicate the reliability of models currently available.

3.5. Gas-phase reaction mechanism 1 (M1)

This first mechanism is based on the well-known detailed scheme developed for isooctane combustion at Lawrence Livermore National Laboratory (LLNL) [19,20], which consists of

4238 reactions among 1034 species, most of them are reversible. This mechanism was later coupled with a detailed toluene scheme from Dagaut et al. [21], which is discussed by Andrae et al. [22]. The toluene mechanism [21] has been validated by experiments of toluene oxidation in an atmospheric jet-stirred reactor, by simulation of benzene oxidation from 0.46 to 10 atm, the ignition of benzene–oxygen–argon mixtures, and the combustion of benzene in flames. The merged mechanism consisted of 8927 reactions among 1082 species.

3.6. Gas-phase reaction mechanism 2 (M2)

A much smaller second mechanism was applied as well. It is derived from various literature sources based on the work by the Dean group [23,24] eventually leading to 3611 reactions among 420 species including the reaction pathway for aromatic and some polyaromatic hydrocarbons, such as naphthalene, anthracene, and pyrene.

4. Results and discussion

4.1. Catalytic case

Exemplarily, the catalytic conversion of isooctane over Rh is discussed at $C/O = 1.1$. At this slightly rich condition, all the oxygen is consumed but conversion of the fuel isooctane is not complete. Rapid catalytic conversion of isooctane basically stops after the first millimeter catalyst (Fig. 1a). In that short entrance zone, not only the major products H_2 and CO but also H_2O and CO_2 (not shown) are formed. The remaining fuel is homogeneously converted by pyrolysis leading to the formation of soot precursors and deposition of carbon on the catalytic surface. At the catalyst exit, significant amounts of ethylene, acetylene, and benzene are predicted, which have also been detected experimentally. However, in the experiment gas-phase reactions may also occur downstream the catalyst, that means the measured data likely differ from the ones occurring at the catalyst exit to a certain amount. The numerically calculated surface coverage of different species along the axial direction for steady state operation of the catalyst shows the formation of a carbon layer on the surface at $z > 1.1$ mm leading to a deactivation of the catalytic surface in this zone (Fig. 2). Since active sites are not available at $z > 1.1$ mm, the inhibiting effect of the noble metal on gas-phase conversion through radical recombination will disappear as well. Consequently, a radical pool can be built-up and homogeneous pyrolysis is likely (Fig. 1b). It should be noted that in real catalytic systems coke formation and build-up is a transient effect overlapping with the catalytic conversion of

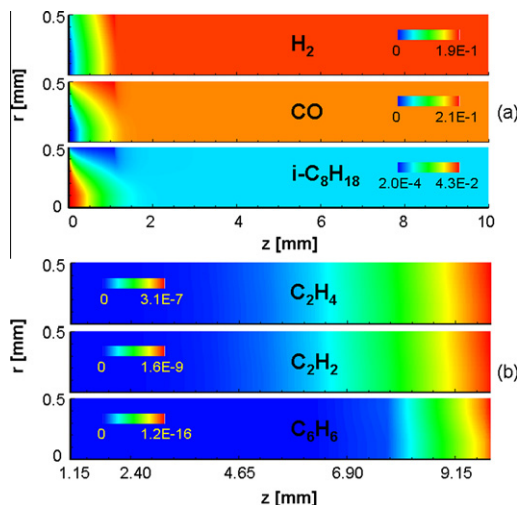


Fig. 1. Numerically predicted mole fractions of iso-octane, CO, H_2 (a) and ethylene, acetylene, and benzene (b) in the catalytic channel at $C/O = 1.1$, 1080 K, 80% N_2 dilution. The symmetry axis of the channel and the gas-wall interface are at $r = 0$ and 0.5 mm, respectively.

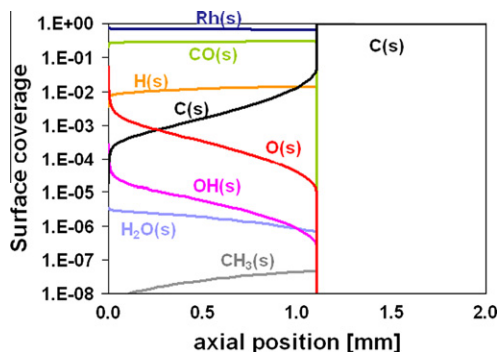


Fig. 2. Numerically predicted surface coverage of adsorbed species as function of axial position along the monolith channel: $C/O = 1.1$, 1080 K, 80% N_2 dilution, 4 SLPM.

hydrocarbon species. The simulation conducted in the present study computes the steady state without taking such transient effects as slow build-up of coke into account, since no model for coke formation was implemented in gas-phase kinetics. The steady-state simulation results show a carbon covered (one monolayer) surface downstream of the reactor, which is consistent with the general experimental observation in CPOX reactors using higher hydrocarbons at rich conditions that the catalyst cokes up starting at the back end of the catalyst. At reaction temperatures above 973 K (700 °C), the simulation and experiments show significant thermal cracking of the fuel.

4.2. Non-catalytic case

The remainder of this paper will now focus on gas-phase reactions only and discuss the potential homogeneous conversion of the remaining fuel in the non-active section of the catalyst and further downstream. The numerically predicted species profiles in the heated empty tube are shown in Fig. 3 at a temperature of 1108 K and rather rich conditions of $C/O = 1.6$. With both chemistry models (M1 and M2), the small (remaining) amount of isooctane is completely converted in the first five millimeters of the reactor. The product composition still varies significantly; even the major products hydrogen and CO vary, their concentrations decrease, while hydrocarbons such as methane, ethylene, propylene, and acetylene are produced. Propylene concentration decreases again ($z > 5$ cm) due to further thermal cracking, hydrogenation, and formation of aromatics and polyaromatics, eventually resulting in carbon deposition. Homogeneous conversion of hydrogen reaches 10% at high temperature and fuel rich conditions whereas CO is only slightly converted (1–2%). Experimental results confirm these trends; for all three C/O ratios studied, hydrogen and carbon monoxide concentrations are slightly reduced, while water and carbon dioxide concentrations increase (except for a gas temperature of 1108 K in case of carbon dioxide). This implies that reverse water-gas shift and hydrogenation reactions here are significant in gas-phase chemistry.

As shown in Fig. 4, significant amounts of C_3 – C_4 olefins (1,2-propadiene, propene, propyne, *n*-butene (1-buten, 2-butene), isobutene, and 1,3-butadiene) are formed directly at the reactor entrance resulting from thermal cracking of the remaining fuel. Ongoing cracking processes combined with acetylene and aromatic hydrocarbons formation farther downstream leads to formation of polyaromatic hydrocarbons like naphthalene,

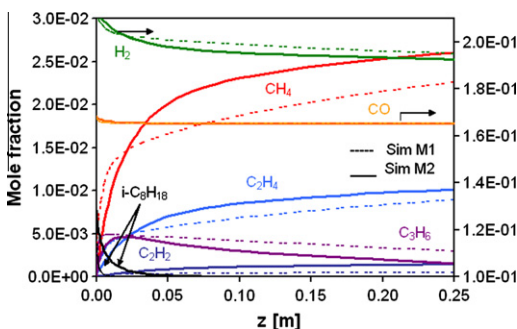


Fig. 3. Numerically predicted fuel and product profiles with mechanisms M1 (dashed lines) and M2 (solid lines) as a function of axial position along the reactor; $C/O = 1.6$, 1108 K, 6 SLPM.

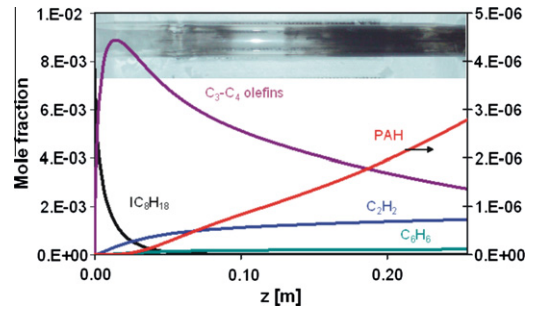


Fig. 4. The distribution of carbon precursors along the reactor modeled with mechanism M2; $C/O = 1.6$, 1108 K, 6 SLPM. C_3 – C_4 olefins contain 1,2-propadiene, propene, propyne, *n*-butene (1-butene, 2-butene), isobutene, 1,3-butadiene; PAH contains naphthalene, anthracene, pyrene. Embedded photo shows the tubular quartz reactor after operation.

anthracene, and pyrene finally resulting in carbon deposition. In the upper part of Fig. 4, a photo of the experimental reactor tube is displayed after operation at these conditions. Two different zones of carbon deposition can clearly be distinguished, a slight carbon zone in the entrance region of the furnace and a pronounced carbon coating around the centre of the reactor. The first carbon deposition results mainly from C_3 – C_4 olefins leading to coke formation via alternative pathways compared to PAH mechanism, while the second carbon deposition arises from continuous PAH formation. The soot formation process in the combustion of hydrocarbons still remains a challenging problem and the mechanism of soot formation is not fully understood. In addition to the mechanism of formation of polyaromatic hydrocarbons some other models have been proposed, such as polyyn model of soot formation, the mechanisms of acetylene pyrolysis and pure carbon cluster formation [25]. One of these alternative pathways can be assumed for coke formation at the first carbon zone. The axial shift in the appearance of the carbon zone in both experiment and simulation likely arises from the not fully adequate assumption of an isothermal reactor, in particular at the inlet at $z = 0$ m. Beyond the first coking zone, no carbon deposits are found, which could be caused by carbon gasification reactions with CO_2 and water and the fact, that olefinic hydrocarbon concentrations are much smaller in this zone whereas the concentration of PAH is not yet large enough for deposit formation.

A minimum reactor temperature is obviously required for thermal cracking processes. In case of isooctane, a temperature of at least 850 K is needed to initiate gas-phase fragmentation and the formation of C_1 – C_3 hydrocarbon species at the given residence time (Fig. 5). Isooctane conversion is not observed below 850 K, neither in

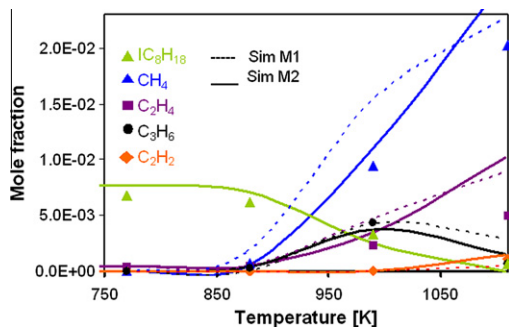


Fig. 5. Product distribution as a function of temperature measured in the center of the reactor tube for $C/O = 1.6$; symbols = experiment, dashed/solid lines = simulations with M1/2.

experiment nor in simulation. With rising temperature more hydrocarbon fragments are produced. A maximum isooctane conversion of 87.5% is observed in case of $C/O = 1.6$ at 1108 K. The main products are methane and propylene for temperatures above 850 K. In the simulation with mechanism M1 more C_1 - C_3 hydrocarbon species are predicted than with M2. This can be related to the missing of PAH formation reactions in M1, in which AH formation only is included. In M2 C_1 - C_3 hydrocarbon species are used for PAH formation resulting in reduced species concentration profiles. The experiment detects even less, indicating that these species have a stronger tendency to form carbon depositions than predicted. When temperature exceeds 990 K, propylene concentration decreases and more ethylene and acetylene are formed, which are not found at temperatures below 1000 K due to its high for-

mation enthalpy. It can be estimated that the consumed amount of propylene is either used for further methane/ethylene formation or for PAH production. Obviously, propylene is preferred instead of ethylene for the allocation of soot precursor species at high temperatures.

Certainly the formation of soot precursor species and therefore carbon deposition does not only depend on reactor temperature but also on gas inlet composition corresponding to different C/O ratios. The higher the C/O inlet ratio, the larger the amount of soot precursors formed. Detailed species profiles in gas-phase reaction as function of C/O ratio at a temperature of 993 K are shown in Fig. 6. Consumption of hydrogen and carbon monoxide slightly rises with increasing C/O ratio; CO reveals a sharper decline than hydrogen for $C/O < 1.3$. The consumption of water and formation of carbon dioxide points to the water-gas shift reaction taking place for $C/O < 1.3$. Figure 6 shows that at higher fuel concentration, $C/O > 1.3$, water is produced but hydrogen increasingly consumed, which is related to methanation.

With the formation of by-products, synthesis gas is consumed by gas-phase reactions. Most of the by-products seem to arise from the fuel via olefin formation. Ethylene does not have a significant influence on gas-phase reaction chemistry as long as isooctane is provided. An increase in ethylene concentration compared to the inlet feed is observed for all C/O ratios and temperatures. Thermal cracking initiates fuel fragmentation at the first millimeters of the reaction zone followed by a variety of reforming and condensations reactions, leading on the one hand to decrease of syngas concentration and on the other hand to PAH formation and finally carbon deposition, both undesired in applications considered.

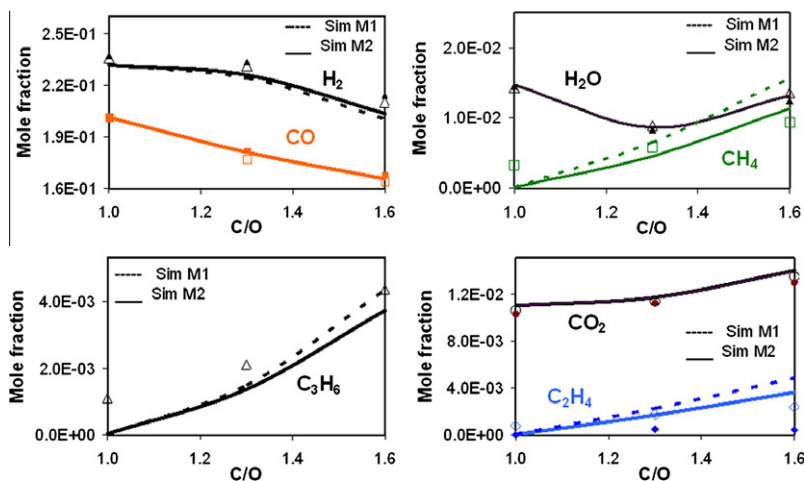


Fig. 6. Species profiles for varying C/O ratio at 993 K; open symbols = experiment, dashed/solid lines = simulations with mechanisms M1/M2, filled symbols = inlet.

5. Conclusions

Isooctane was chosen as model substance to better understand the impact of gas-phase reactions on conversion and selectivity in CPOX of logistic fuels. At rich conditions, i.e. molar C/O ratios above unity, the catalyst is covered by carbon deposits downstream the position, at which all oxygen is consumed. In this catalyst zone and downstream the catalyst, gas-phase reactions play a major role in conversion of the remaining fuel. Pure gas-phase experiments and simulations with two different large elementary-step experiments reveal: apart from surface reactions, gas-phase reactions among a multitude of species is responsible for coke formation when unconverted fuel leaves the high temperature oxidation zone in the catalyst. Large amounts of olefinic hydrocarbons are initially formed by thermal cracking leading to aromatic molecules and PAHs. The presence of gas-phase reactions in the post-catalytic zone decreases the amount of hydrogen produced through methanation and hydrogenation of carbon monoxide and olefins, especially at fuel rich conditions. The cracking of remaining fuel increases the concentration of by-products (ethylene, acetylene, and C₃–C₄ olefins) and as a consequence of carbon deposits.

This study also reveals that experimentally determined yields (major as well as minor products) in laboratory CPOX reactors may deviate from the local yields at the catalyst exit, because the products can usually not be quenched sufficiently fast to avoid gaseous post-reactions occurring within millimeters beyond the catalyst. Models can here be used to re-calibrate the measured data by solving the inverse problem of determining what concentration would have existed at the catalyst exit. While such an approach will be usable only in special cases, an estimation of the impact of gas-phase reactions on the conversion in catalytic reforming of gasoline and diesel fuel can support design and optimization of technical fuel reformers.

Even though both gas-phase reaction models and the surface reaction model are able to predict the species profiles well, several unresolved issues remain such as the reactions between gas-phase species and the carbon-coated catalyst and the temporal effects, e.g. the rate of loss of catalytic activity with increasing carbon deposition.

References

- [1] C.E. Thomas, B.D. James, F.D. Lomax, I.F. Kuhn Jr., *Int. J. Hydrogen Energy* 25 (2000) 551–567.
- [2] S. Ahmed, M. Krumpelt, *Int. J. Hydrogen Energy* 26 (2001) 291–301.
- [3] N. Burke, D. Trimm, *React. Kinet. Catal. Lett.* 84 (2005) 137–142.
- [4] R. Schwiedernoch, S. Tischer, C. Correa, O. Deutschmann, *Chem. Eng. Sci.* 58 (2003) 633–642.
- [5] C. Appel, J. Mantzaras, R. Schaeren, R. Bombach, A. Inauen, N. Tylli, M. Wolf, T. Griffin, D. Winkler, R. Carroni, *Proc. Combust. Inst.* 30 (2005) 2509–2517.
- [6] A. Schneider, J. Mantzaras, R. Bombach, S. Schenker, N. Tylli, P. Jansohn, *Proc. Combust. Inst.* 31 (2007) 1973–1981.
- [7] R. Horn, N.J. Degenstein, A.K. Williams, L.D. Schmidt, *Catal. Lett.* 110 (2006) 169–178.
- [8] R. Schwiedernoch, S. Tischer, H.-R. Volpp, O. Deutschmann, *Natural Gas Conversion VII*, in: Xinhe Bao, Yide Xu (Eds.), *Stud. Surf. Sci. Catal.* 147, Elsevier, 2004, pp. 511–516.
- [9] A.K. Williams, R. Horn, L.D. Schmidt, *AIChE J.* 53 (2007) 2097–2113.
- [10] M. Hartmann, S. Lichtenberg, N. Hebben, D. Zhang, O. Deutschmann, *Chem. Ing. Tech.* 81 (2009) 909–919.
- [11] M. Hartmann, T. Kaltschmitt, O. Deutschmann, *Catal. Today* 147 (Suppl 1) (2009) S204–S209.
- [12] M. Hartmann, L. Maier, H.D. Minh, O. Deutschmann, *Combust. Flame* 157 (2010) 1771–1782.
- [13] O. Deutschmann, S. Tischer, S. Kleditzsch, et al., DETCHEM™ software package, version 2.2, Karlsruhe, 2008, <<http://www.detchem.com>>.
- [14] O. Deutschmann, R. Schwiedernoch, L.I. Maier, D. Chatterjee, *Natural Gas Conversion VI*, in: E. Iglesia, J.J. Spivey, T.H. Fleisch (Eds.), *Stud. Surf. Sci. Catal.*, 136, Elsevier, 2001, pp. 251–258.
- [15] D.K. Zerkle, M.D. Allendorf, M. Wolf, O. Deutschmann, *J. Catal.* 196 (2000) 18–39.
- [16] J. Thormann, L. Maier, P. Pfeifer, U. Kunz, K. Schubert, O. Deutschmann, *Int. J. Hydrogen Energy* 34 (2009) 5108–5120.
- [17] H.D. Minh, H.G. Bock, S. Tischer, O. Deutschmann, *AIChE J.* 54 (2008) 2432–2440.
- [18] L.L. Raja, R.J. Kee, O. Deutschmann, J. Warnatz, L.D. Schmidt, *Catal. Today* 59 (2000) 47–60.
- [19] H.J. Curran, P. Gaffuri, W.J. Pitz, C.K. Westbrook, *Combust. Flame* 129 (3) (2002) 253–280.
- [20] http://www.cms.llnl.gov/combustion/combustion_home.html.
- [21] P. Dagaut, G. Pengloan, A. Ristori, *Phys. Chem. Chem. Phys.* 4 (2002) 1846–1854.
- [22] J. Andrae, D. Johansson, P. Björnbohm, P. Risberg, G. Kalghatgi, *Combust. Flame* 140 (2005) 267–286.
- [23] C.A. Mims, R. Mauti, A.M. Dean, K.D. Rose, *J. Phys. Chem.* 98 (50) (1994) 13357–13372.
- [24] K.M. Walters, A.M. Dean, H. Zhu, R.J. Kee, *J. Power Sources* 123 (2003) 182–189.
- [25] P.A. Vlasov, J. Warnatz, *Proc. Combust. Inst.* 29 (2002) 2335–2341.